



Temperature-feedback two-photon-responsive metal-organic frameworks for efficient photothermal therapy

Xianshun Sun^{1*}, Xin Lu^{2*}, Wenyao Duan^{2*}, Bo Li², Yupeng Tian¹, Dandan Li² , and Hongping Zhou¹ 

¹School of Chemistry and Chemical Engineering, Anhui University, Hefei 230601, China;

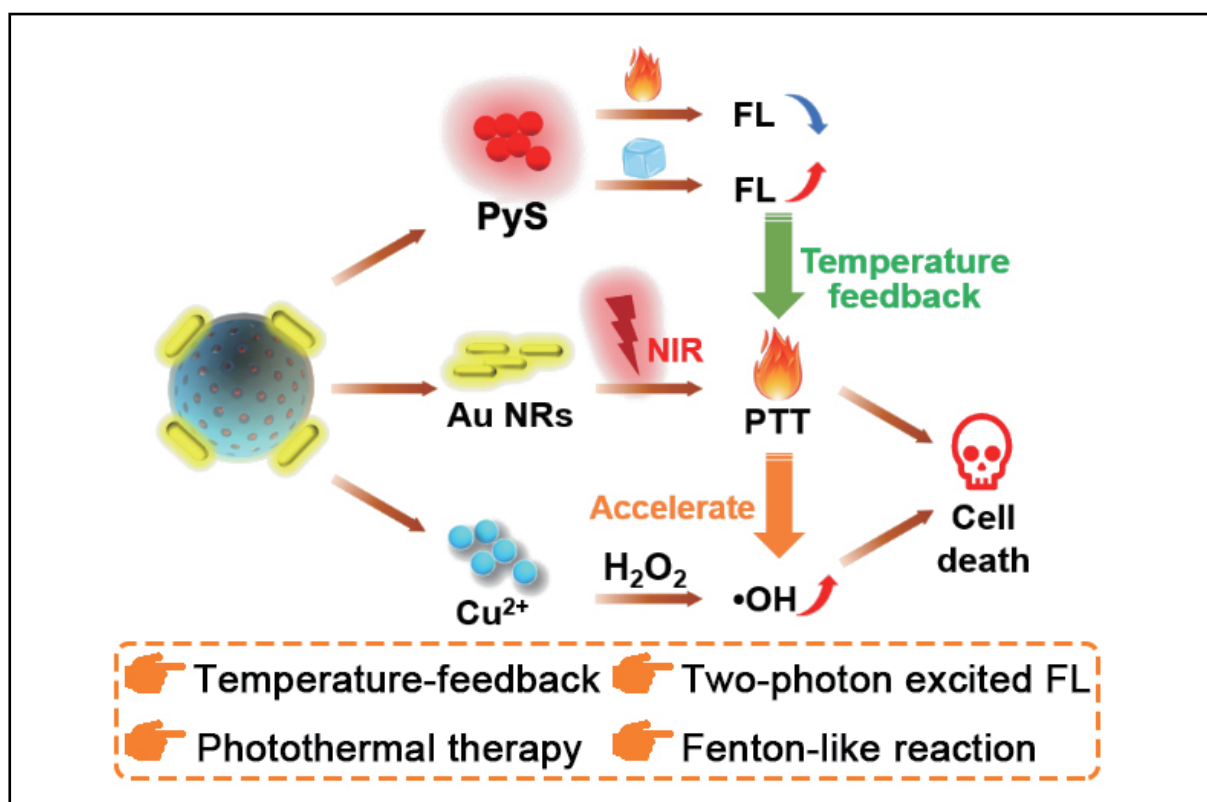
²Institutes of Physical Science and Information Technology, Key Laboratory of Structure and Functional Regulation of Hybrid Materials, Ministry of Education, Anhui University, Hefei 230601, China

* These authors contributed equally to this work

 Correspondence: Dandan Li, E-mail: chemlidd@163.com; Hongping Zhou, E-mail: zhpzhp@263.net

© 2024 The Author(s). This is an open access article under the CC BY-NC-ND 4.0 license (<http://creativecommons.org/licenses/by-nc-nd/4.0/>).

Graphical abstract





Schematic illustration of temperature-sensitive photothermal therapy and promoted chemodynamic therapy.

Public summary

- AMPP demonstrated near-infrared light induced two-photon responsive temperature-feedback for efficient photothermal therapy.
- AMPP displayed excellent photothermal therapy efficiency under 900 nm laser irradiation.
- The Fenton-like reaction generated from the degradation of MOF-199 can be accelerated by increasing the temperature during the photothermal therapy process.

Temperature-feedback two-photon-responsive metal-organic frameworks for efficient photothermal therapy

Xianshun Sun^{1*}, Xin Lu^{2*}, Wenyao Duan^{2*}, Bo Li², Yupeng Tian¹, Dandan Li² , and Hongping Zhou¹ 

¹School of Chemistry and Chemical Engineering, Anhui University, Hefei 230601, China;

²Institutes of Physical Science and Information Technology, Key Laboratory of Structure and Functional Regulation of Hybrid Materials, Ministry of Education, Anhui University, Hefei 230601, China

* These authors contributed equally to this work

 Correspondence: Dandan Li, E-mail: chemlidd@163.com; Hongping Zhou, E-mail: zhpzhp@263.net

© 2024 The Author(s). This is an open access article under the CC BY-NC-ND 4.0 license (<http://creativecommons.org/licenses/by-nc-nd/4.0/>).

 Cite This: *JUSTC*, 2024, 54(6): 0608 (7pp)

 Read Online

 Supporting Information

Abstract: The realization of real-time thermal feedback for monitoring photothermal therapy (PTT) under near-infrared (NIR) light irradiation is of great interest and challenge for antitumor therapy. Herein, by assembling highly efficient photothermal conversion gold nanorods and a temperature-responsive probe ((E)-4-(4-(diethylamino)styryl)-1-methylpyridinium, PyS) within MOF-199, an intelligent nanoplatform (AMPP) was fabricated for simultaneous chemodynamic therapy and NIR light-induced temperature-feedback PTT. The fluorescence intensity and temperature of the PyS probe are linearly related due to the restriction of the rotation of the characteristic monomethine bridge. Moreover, the copper ions resulting from the degradation of MOF-199 in an acidic microenvironment can convert H₂O₂ into •OH, resulting in tumor ablation through a Fenton-like reaction, and this process can be accelerated by increasing the temperature. This study establishes a feasible platform for fabricating highly sensitive temperature sensors for efficient temperature-feedback PTT.

Keywords: metal-organic framework; two-photon; temperature feedback; photothermal therapy; chemodynamic therapy

CLC number: TB383; R730.5

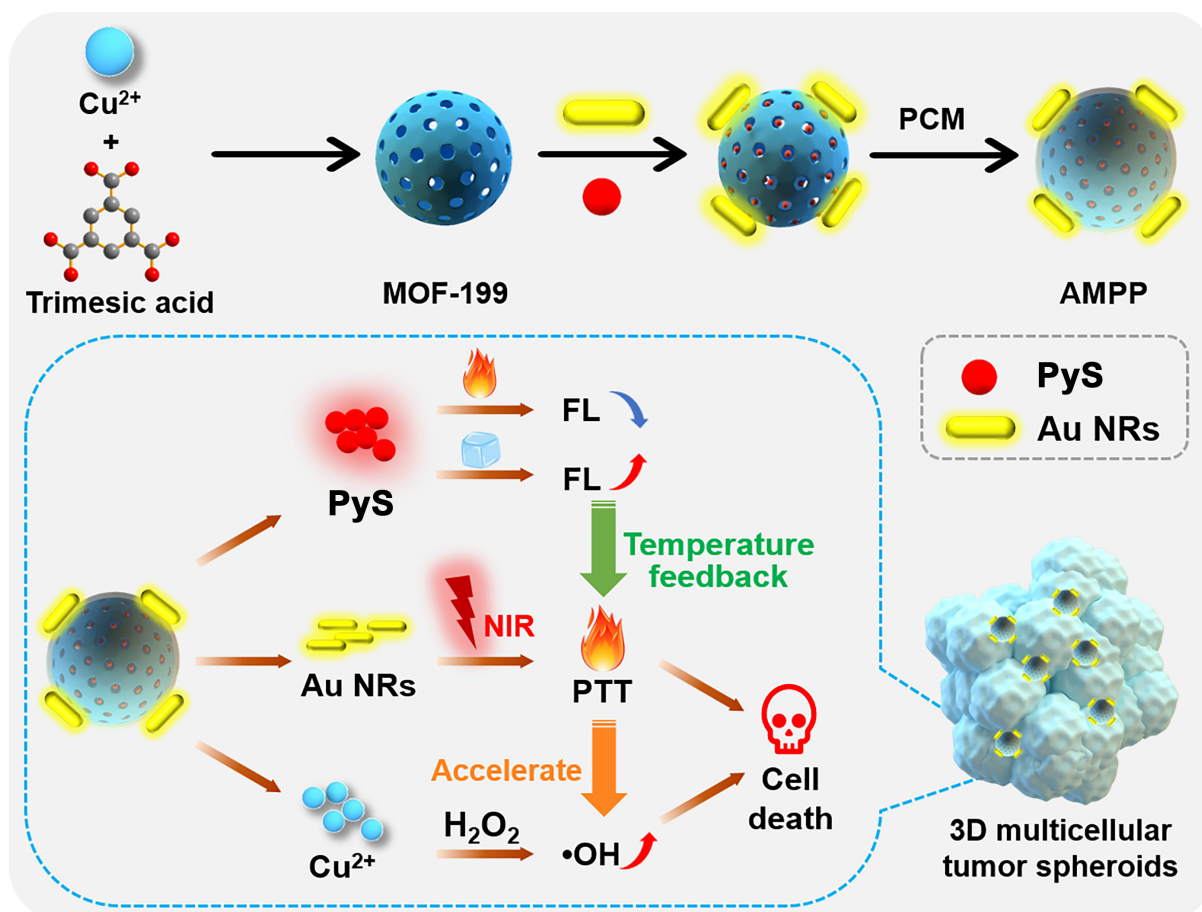
Document code: A

1 Introduction

Photothermal therapy (PTT) converts light into thermal energy to achieve efficient cancer therapy and is considered to be an effective approach due to its noninvasive and spatiotemporal control abilities^[1–3]. In this process, photothermal agents (PTAs) generate hyperthermia upon light irradiation, which can ablate cancer cells. Importantly, real-time temperature monitoring plays a vital role during PTT^[4]. Cancer cells cannot be killed effectively at a lower temperature (lower than 45 °C), while rapid heating or excessive temperature adversely initiates an undesirable cell death process that can potentially induce cancer metastasis and inflammatory disease^[5–7]. To solve this problem, fluorescence thermometry has been promoted as a noninvasive method that shows a rapid response and high sensitivity to the intracellular temperature. However, the excitation wavelengths of most fluorescence thermometers are in the ultraviolet–visible region, which restricts their applications because of their cytotoxicity, photobleaching and autofluorescence^[8]. Since excited wavelengths are usually located in the near-infrared (NIR) region, two-photon excited fluorescence probes have been widely used due to their strong ability to penetrate tissues, weak scattering effect and reduced photobleaching effect^[9], making them promising candidates for temperature sensors. As a consequence, it is highly important to construct a two-photon fluorescent probe platform for real-time temperature monitoring to avoid hyperthermia during PTT.

Although significant progress has been made in the design of temperature-feedback fluorescent probes, most of these organic probes suffer from fluorescence quenching and low tumor targeting. To solve these problems, metal-organic frameworks (MOFs) can be used as carriers because of their unique structures. MOFs are a class of nanomaterials with abundant pores and large surface areas that have been widely used for catalysis, gas storage, optical sensors and cancer therapy^[10–12]. Most importantly, the pore confinement of MOFs endows them with a very promising platform for guest encapsulation^[13,14]. In this sense, MOFs are promising candidates for use as carriers for drug delivery.

Keeping the above points in mind, we designed an intelligent MOF-based nanoplatform for real-time monitoring of cell temperature during the NIR light-induced PTT process (Scheme 1). MOF-199 [Cu₃(TMA)₂(H₂O)₃]_n was chosen as a nanocarrier, and the photothermal agent gold nanorods (Au NRs) and temperature-responsive pyridinium salt molecules (PyS) were simultaneously loaded to realize noninvasive therapy under the guidance of real-time temperature. Herein, the fabrication of the nanoplatform (denoted as AMPP) is based on the following considerations: (i) two-photon responsive PyS can realize real-time temperature monitoring under NIR light irradiation, and the coated phase-change material (PCM, 1-tetradecanol) film can effectively prevent the leakage of PyS and achieve temperature-controlled release^[15,16]; (ii) Au NRs with high photothermal conversion efficiency can realize PTT under NIR light irradiation, and localized hyperthermia



Scheme 1. Schematic illustration showing the preparation of AMPP, highlighting the process of temperature-sensitive photothermal therapy and promoted chemodynamic therapy.

can further accelerate •OH generation for enhanced chemodynamic therapy (CDT); and (iii) MOF-199 is degraded in the acidic tumor microenvironment, and the released copper ions can react with the overexpressed H₂O₂ to generate •OH through a Fenton-like reaction to realize CDT. The results demonstrated that the AMPP nanoplateform can not only accomplish real-time precise monitoring of cancer cell temperature but also cooperate with PTT and CDT to achieve synergistic anticancer therapy.

2 Materials and methods

Synthesis of PyS. PyS was synthesized according to the literature^[17]. ¹H NMR (400 MHz, acetone-*d*₆) δ 8.85 (d, *J*=6.2 Hz, 2H), 8.64 (d, *J*=6.4 Hz, 1H), 7.88 (d, *J*=6.0 Hz, 1H), 7.63–7.51 (m, 2H), 7.13 (d, *J*=6.0 Hz, 1H), 6.84–6.68 (m, 2H), 3.47 (q, *J*=7.0 Hz, 6H).

Synthesis of MOF-199. Cu(NO₃)₂ (0.9 mL, 0.2 mol·L⁻¹), hexadecyl trimethyl ammonium bromide (9.6 mL, 0.2 mol·L⁻¹) and benzene-1,3,5-tricarboxylate triethylammonium salt (0.6 mL, 0.2 mol·L⁻¹) were stirred vigorously for 2 min and centrifuged to obtain MOF-199.

Synthesis of Au NRs. Au NRs were synthesized through a seed-driven growth method^[18]. CTAB solution (10.0 mL, 0.10 mol·L⁻¹), HAuCl₄ (0.1 mL, 2.5 × 10⁻⁴ mol·L⁻¹) and frozen NaBH₄ (0.6 mL, 0.02 mol·L⁻¹) were mixed. In a 250 mL flask, CTAB (50 mL, 0.1 mol·L⁻¹), AgNO₃ (0.6 mL, 4 × 10⁻³

mol·L⁻¹) and HAuCl₄ (1.0 mL, 2.5 × 10⁻⁴ mol·L⁻¹) were mixed, stirred for 2 min and stored for 2 h at 28 °C to prepare the raw growth liquid. AA (0.6 mL, 0.08 mol·L⁻¹) was gradually added until the solution became colorless. After adding 0.1 mL of seed fluid at 28 °C, the color gradually changed. The Au NRs were preserved for 12 h and collected after centrifugation.

Synthesis of AMPP. The synthesized MOF-199 (5 mg) and PyS (5 mg) were mixed and stirred for 6 h at 25 °C, and then, the dispersed Au NRs were added and stirred for 6 h. Finally, PCM (15 mg) was added to the solution, which was subsequently stirred for 3 min, centered at 8000 r/min for 1 min and washed with methanol 3 times.

3 Results and discussion

3.1 Characterization of AMPP

Defective MOF-199, which acts as a carrier, was initially synthesized according to our previous work^[19], and its morphology was observed through scanning electron microscopy (SEM) images (Fig. 1a). The embedded fluorescent sensor candidate (E)-4-(4-(diethylamino)styryl)-1-methylpyridin-1-ium (PyS) was prepared through a condensation reaction, as shown in Figs. S1 and S2. Moreover, highly uniform Au NRs with an average diameter of 50 nm were prepared (Fig. 1b). Then, MOF-199 loaded with PyS and Au NRs was synthe-

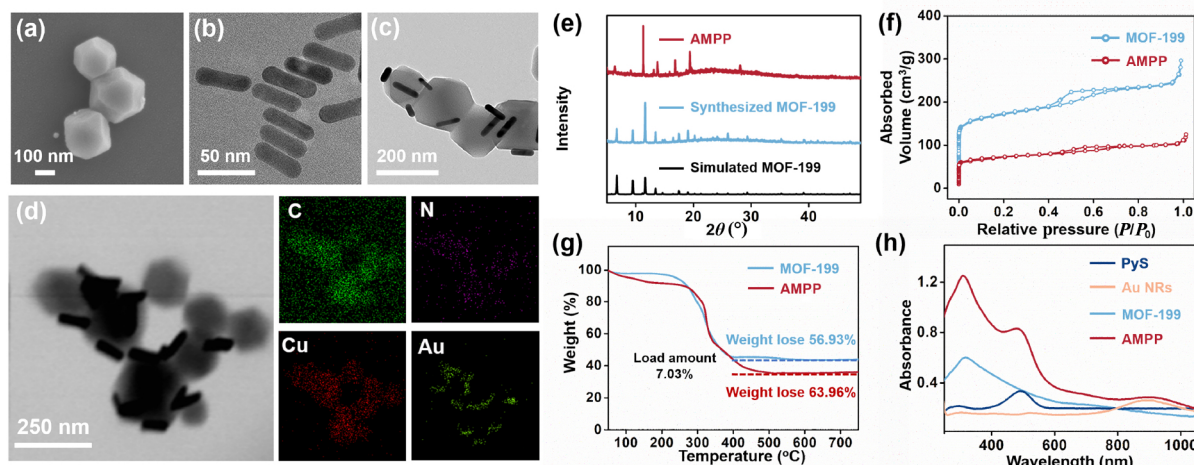


Fig. 1. (a) SEM image of MOF-199. (b) TEM image of the Au NRs. (c) TEM image of AMPP. (d) TEM image and elemental mapping of AMPP. (e) Powder XRD patterns of simulated MOF-199, synthesized MOF-199 and AMPP. (f) BET results of MOF-199 and AMPP. (g) TGA curves of MOF-199 and AMPP. (h) UV-vis absorption spectra of PyS, the Au NRs, MOF-199 and AMPP. Concentration: 100 $\mu\text{g}\cdot\text{mL}^{-1}$; solvent: deionized water.

ized via a one-pot method. Finally, AMPP was obtained with 1-tetradecanol as a PCM to achieve the controlled release of PyS through coating on the surface of MOF-199 (Fig. 1c). Obviously, the elemental mapping analysis of AMPP (Fig. 1d) illustrated that the materials were successfully fabricated, and the obtained AMPP exhibited high crystallinity according to the powder XRD patterns (Fig. 1e). Furthermore, zeta potential analysis revealed distinct variations in the ζ -potentials from +11.58 mV (MOF-199) to -1.49 mV (AMPP), further indicating the successful fabrication of AMPP (Fig. S3). The obtained AMPP showed similar N_2 isotherms at 77 K to those of MOF-199 (Fig. 1f), and the decreased N_2 sorption and pore volume of AMPP compared with those of pristine MOF-199 could be ascribed to the loading of PyS and Au NRs. As illustrated in Fig. 1g, the weight loss between 400 $^{\circ}\text{C}$ and 750 $^{\circ}\text{C}$ can be attributed to the decomposition of PyS, and the loading efficiency of PyS was calculated to be 7.03% according to TGA measurements of AMPP. In addition, the obtained materials exhibited obvious absorption bands for MOF-199, PyS and Au NRs (Fig. 1h), illustrating the successful synthesis of AMPP.

3.2 Two-photon thermal responsive properties

Notably, the absorption band of the obtained AMPP was located in the near-infrared optical window (absorption peak: 900 nm; Fig. 1h), implying its considerable photothermal conversion efficiency for PTT. Importantly, its temperature sensitivity upon NIR light irradiation plays a vital role in real-time temperature feedback during PTT. Herein, the rotation of the characteristic monomethine bridge in the embedded fluorescent probe PyS can be regulated by the ambient temperature, resulting in emission activation or deactivation (Fig. 2a)^[20]. Moreover, the typical D- π -A structure of the probe PyS endows it with considerable two-photon activity (Fig. S4). Based on the above features, we investigated the response of the two-photon excited fluorescence of PyS upon 900 nm laser excitation to temperature (Fig. 2b). Obviously, the fluorescence intensity gradually decreased as the temperature increased from 25 $^{\circ}\text{C}$ to 50 $^{\circ}\text{C}$, and the fluorescence variation exhibited a linear relationship with that of the ambient

temperature (Fig. S5), indicating the temperature sensing ability of the embedded fluorescent probe PyS. Accordingly, as shown in Figs. 2c–2f and S6, AMPP exhibited considerable two-photon excited fluorescence under 900 nm excitation, and the intensity decreased linearly as the temperature increased from 25 $^{\circ}\text{C}$ to 50 $^{\circ}\text{C}$ (physiological temperature region), making it a valid NIR light-responsive temperature sensor. Fig. S7 (thermally responsive release rate of PyS) shows that the release of the fluorescent probe PyS could be controlled by temperature. These results indicate that the system can realize NIR light-induced two-photon fluorescence physiological temperature sensing, which offers ample possibilities for temperature-feedback PTT treatment.

3.3 Photothermal properties of AMPP under NIR laser irradiation

Motivated by the successful fabrication of the temperature-responsive platform, the photothermal conversion capability of AMPP was investigated under NIR laser (900 nm) irradiation. As shown in Fig. 3a and b, the photothermal conversion temperature of AMPP exceeded 45 $^{\circ}\text{C}$ (the lowest temperature for killing cancer cells and inducing apoptosis), and its photothermal conversion efficiency was calculated to be 58.3%^[21], indicating its potential as a photothermal agent (Fig. 3c). In addition, the thermal images collected under 900 nm irradiation using a near-infrared thermal camera further demonstrated the above issue (Fig. 3d). AMPP showed negligible changes after three heating/cooling cycles, indicating its high photothermal stability (Fig. S8). Moreover, the Cu ions released from the degradation of MOF-199 in an acidic environment could trigger $\cdot\text{OH}$ generation through a Fenton-like reaction. Additionally, the increased temperature induced by light can actually improve the generation efficiency of $\cdot\text{OH}$ for enhanced CDT.

3.4 Photothermal properties of AMPP in vitro

To further validate the potential of AMPP as a temperature-sensitive photothermal agent, we evaluated its NIR light-induced imaging and apoptosis ability using confocal laser scanning microscopy (CLSM). As shown in Fig. S11, the

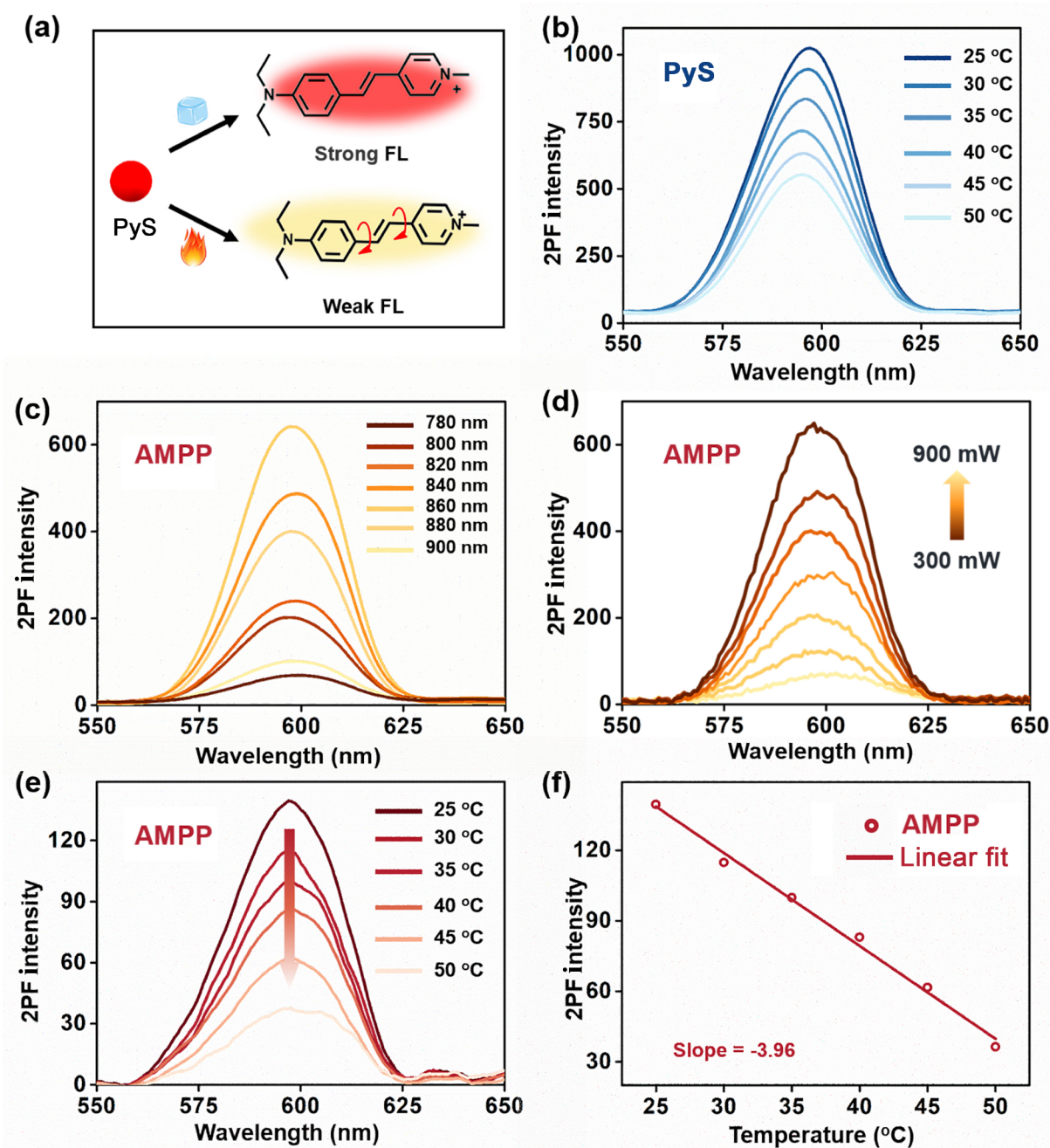


Fig. 2. (a) Illustration of the changes in the fluorescence intensity of PyS with temperature. (b) Two-photon excited fluorescence performance of PyS upon 900 nm laser excitation at different temperatures (concentration: 1 mmol·L⁻¹; solvent: PBS; temperature: 25 °C, 30 °C, 35 °C, 40 °C, 45 °C, 50 °C). (c) Two-photon excited fluorescence spectrum of AMPP (concentration: 150 μg·mL⁻¹; solvent: PBS; wavelength: 780–900 nm). (d) Two-photon excited fluorescence spectrum of AMPP upon 900 nm laser excitation with different input powers (concentration: 150 μg·mL⁻¹; solvent: PBS; power: 300–900 mW). (e) Two-photon excited fluorescence spectrum of AMPP upon 900 nm laser excitation at different temperatures (concentration: 150 μg·mL⁻¹; solvent: PBS; temperature: 25 °C, 30 °C, 35 °C, 40 °C, 45 °C, 50 °C). (f) The linear relationship between temperature and two-photon fluorescence intensity for AMPP.

evident red fluorescence observed in HepG2 cells confirmed the effective accumulation of AMPP, facilitating further intracellular experiments. Motivated by the excellent linear relationship between fluorescence and temperature under NIR light irradiation of AMPP, we conducted temperature-feedback experiments in HepG2 cells excited by 513 nm and 900 nm lasers. As depicted in Fig. 4a, after irradiation at 900 nm for 60 s, the fluorescence intensity decreased by approximately 74.60%, while no significant changes were observed

under 513 nm laser irradiation. The corresponding temperature can be calculated through the linear fit curve, enabling temperature detection through fluorescence intensity (Fig. 2f). To further confirm the intracellular generation of •OH by AMPP, aminophenyl fluorescein (APF) was employed as a detector. As shown in Fig. 4b, the APF signal increased after incubation with H₂O₂, indicating the generation of •OH by Fenton-like reactions. Additionally, the amplified fluorescence of APF under NIR laser irradiation enhanced the •OH

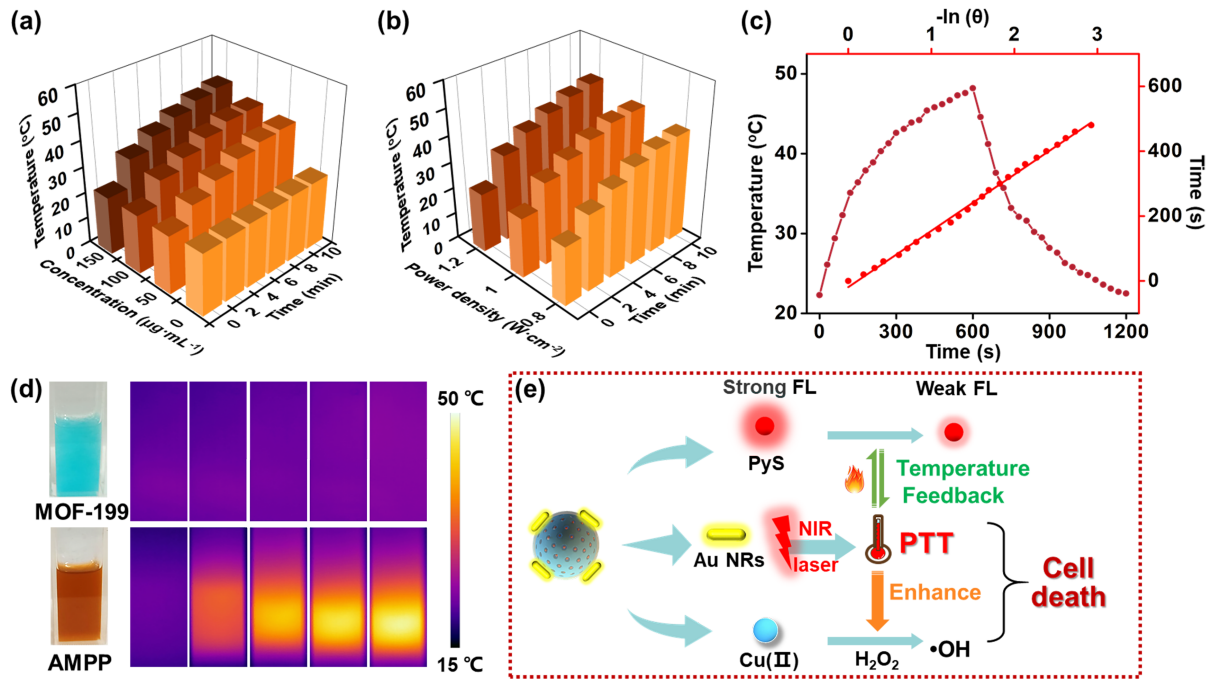


Fig. 3. (a) The temperature variation of AMPP with different concentrations under NIR light (900 nm, 1.0 W·cm⁻²) for 10 min. (b) The temperature variation of AMPP with different input power densities under 900 nm (1.0 W·cm⁻²) laser irradiation for 10 min. (c) Photothermal conversion performance of AMPP (150 μg·mL⁻¹) obtained from linear time data vs. -ln(θ) from the cooling period. (d) Infrared thermal images of MOF-199 (150 μg·mL⁻¹) and AMPP (150 μg·mL⁻¹) under 900 nm laser irradiation (1.0 W·cm⁻²). (e) Schematic illustration showing the temperature feedback and therapeutic process of AMPP.

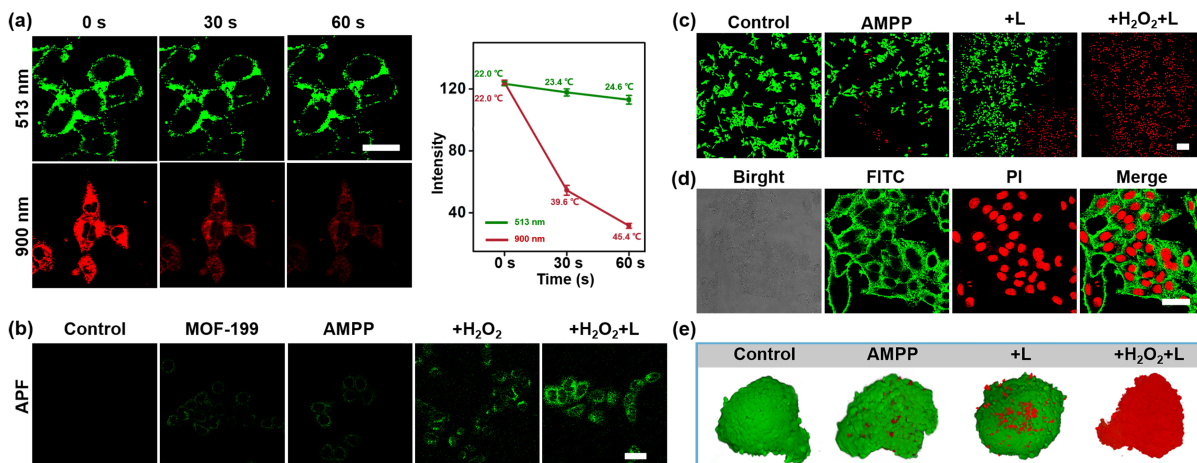


Fig. 4. (a) Fluorescence intensity of AMPP within HepG2 cells under 513 nm and 900 nm laser irradiation. Right: the fluorescence intensity and corresponding temperature under different irradiation times. (b) CLSM images of HepG2 cells treated with AMPP (150 μg·mL⁻¹), and APF was used to detect the generation of •OH (AMPP: 150 μg·mL⁻¹; H₂O₂: 100 μmol·L⁻¹; scale bar: 25 μm). (c) CLSM images of AMPP-treated HepG2 cells stained with calcein-AM/PI (laser: 900 nm, 0.1 W·cm⁻²; AMPP: 150 μg·mL⁻¹; H₂O₂: 100 μmol·L⁻¹; scale bar: 100 μm). (d) AMPP-incubated HepG2 cells were stained with Annexin V-FITC/PI after irradiation (laser: 900 nm, 0.1 W·cm⁻²; AMPP: 150 μg·mL⁻¹; scale bar: 25 μm). (e) 3D fluorescence images of MCTs subjected to different treatments (laser: 900 nm, 0.1 W·cm⁻²; AMPP: 150 μg·mL⁻¹; H₂O₂: 100 μmol·L⁻¹).

level, corroborating the process of thermopromoted Fenton-like reactions.

Next, we evaluated the phototoxicity efficiency of AMPP using (4,5-dimethylthiazol-2-yl)-2,5-diphenyltetrazolium bromide (MTT) assays. As depicted in Fig. S12, no obvious cell death was observed after incubation with AMPP for 12 h, indicating its low dark cytotoxicity. However, when light irradiation and H₂O₂ were added, the viability of HepG2 cells decreased significantly. Notably, the group treated with AMPP

combined with light and H₂O₂ showed much lower cell viability (approximately 10%), demonstrating excellent synergistic therapeutic efficacy. Furthermore, preliminary tests were conducted to detect cell death using a live/dead cell staining assay, in which calcein-AM/propidium iodide (PI) was applied to stain live and dead cells with green and red fluorescence, respectively (Fig. 4c). These results further indicated the in vitro combination of PTT and CDT of AMPP. In addition, the apoptosis induced by AMPP was assayed by CLSM

and flow cytometry analysis with annexin-V-FITC (fluorescein isothiocyanate) and PI (propidium iodide) (Figs. 4d and S13). The fraction of late apoptotic cells increased with H₂O₂ and NIR light irradiation (97.6%), consistent with the results of the MTT and FITC/PI assays. Moreover, we applied Hep G2 3D multicellular tumor spheroids (3D MCTs), a more representative model of clinically treated tumors, to confirm the NIR light-induced PTT and synergetic enhanced CDT efficiency in deep cancer tissue. The 3D MCTs were first incubated with AMPP and calcein-AM/PI to measure viability and apoptosis in real time. As shown in Fig. 4e, the 3D MCTs formed distinct necrotic nuclei under NIR irradiation and H₂O₂ treatment compared to those in the control group. The bright red fluorescence confirmed the apparent synergistic therapeutic effect, demonstrating that AMPP can be employed as a PTT and CDT combination therapy platform.

4 Conclusions

In conclusion, an intelligent nanoplatform (AMPP) that can realize in situ real-time temperature feedback during noninvasive PTT under NIR laser irradiation was fabricated. Benefiting from the successful loading of a two-photon responsive probe (PyS) and Au NRs, AMPP exhibited outstanding temperature responsiveness and excellent photothermal conversion efficiency (58.3%) under NIR light irradiation (900 nm). In addition, MOF-199 can induce apoptosis through the CDT process, which can be accelerated by local hyperthermia during the photothermal process, synergistically realizing effective tumor ablation. In addition, AMPP has been demonstrated to be a valid therapeutic agent both in vitro and in vivo. Overall, this work provides a promising platform for the construction of a two-photon responsive system for temperature-feedback PTT and the enhancement of CDT.

Supporting information

The supporting information for this article can be found online at <https://doi.org/10.52396/JUSTC-2024-0005>. The supplemental information includes 13 figures. General experimental details, synthetic procedures, characterization data, zeta potentials, two-photon fluorescence spectra, release ability of PyS, temperature curves, MB degradation, ESR spectra, CLSM images, and cell viability and flow cytometry apoptosis assay are provided in the supporting information.

Acknowledgements

This work was supported by the National Natural Science Foundation of China (22171001, 22305001, 51972001, 52372073) and the Natural Science Foundation of Anhui Province of China (2108085MB49).

Conflict of interest

The authors declare that they have no conflict of interest.

Biographies

Xianshun Sun is currently a lecturer in the School of Chemistry and Chemical Engineering, Anhui University. He received his Ph.D. degree

from the University of Science and Technology of China in 2020. His research primarily revolves around the development of two-dimensional materials for biological applications.

Xin Lu is currently a post-doctoral researcher in the Institutes of Physical Science and Information Technology, Anhui University. She received her Ph.D. degree from Anhui University in 2022. Her research mainly focuses on the study and development of multiphoton absorption materials.

Wenyao Duan received his master's degree from Anhui University in 2023, under the supervision of Dr. Dandan Li. His research mainly focuses on the investigation of multiphoton responsive metal-organic frameworks.

Dandan Li is currently an Associate Professor in the Institutes of Physical Science and Information Technology, Anhui University. She received her Ph.D. degree from Anhui University in 2016. Her research primarily revolves around the fabrication of multiphoton absorption materials for biological applications.

Hongping Zhou is currently a Professor in the School of Chemistry and Chemical Engineering, Anhui University. She received her Ph.D. degree from the University of Science and Technology of China in 2006. Her research primarily centers around the fabrication of fluorescent organic probes for biological applications.

References

- [1] Chen J J, Zhu Y F, Wu C T, et al. Nanoplatform-based cascade engineering for cancer therapy. *Chemical Society Reviews*, **2020**, *49* (24): 9057–9094.
- [2] Yin N, Wang Y H, Huang Y, et al. Modulating nanozyme-based nanomachines via microenvironmental feedback for differential photothermal therapy of orthotopic gliomas. *Advanced Science*, **2023**, *10* (3): 2204937.
- [3] Wang Z, Sun Q Q, Liu B, et al. Recent advances in porphyrin-based MOFs for cancer therapy and diagnosis therapy. *Coordination Chemistry Reviews*, **2021**, *439*: 213945.
- [4] Yang K, Zhao S J, Li B L, et al. Low temperature photothermal therapy: Advances and perspectives. *Coordination Chemistry Reviews*, **2022**, *454*: 214330.
- [5] Meng X F, Zhang B Y, Yi Y, et al. Accurate and real-time temperature monitoring during MR imaging guided PTT. *Nano Letters*, **2020**, *20* (4): 2522–2529.
- [6] Xu M Z, Xue B, Wang Y, et al. Temperature-feedback nanoplatform for NIR-II penta-modal imaging-guided synergistic photothermal therapy and CAR-NK immunotherapy of lung cancer. *Small*, **2021**, *17* (43): 2101397.
- [7] Yoo D, Jeong H, Noh S H, et al. Magnetically triggered dual functional nanoparticles for resistance-free apoptotic hyperthermia. *Angewandte Chemie International Edition*, **2013**, *52* (49): 13047–13051.
- [8] Feng T T, Ye Y X, Liu X, et al. A robust mixed-lanthanide polyMOF membrane for ratiometric temperature sensing. *Angewandte Chemie International Edition*, **2020**, *59* (48): 21752–21757.
- [9] Shen F F, Chen Y, Xu X F, et al. Supramolecular assembly with near-infrared emission for two-photon mitochondrial targeted imaging. *Small*, **2021**, *17* (30): 2101185.
- [10] Wen L L, Sun K, Liu X S, et al. Electronic state and microenvironment modulation of metal nanoparticles stabilized by MOFs for boosting electrocatalytic nitrogen reduction. *Advanced Materials*, **2023**, *35* (15): 2210669.
- [11] Gutiérrez M, Zhang Y, Tan J C. Confinement of luminescent guests in metal-organic frameworks: understanding pathways from

- synthesis and multimodal characterization to potential applications of LG@MOF systems. *Chemical Reviews*, **2022**, *122* (11): 10438–10483.
- [12] Li B, Lu X, Tian Y P, et al. Embedding multiphoton active units within metal–organic frameworks for turning on high-order multiphoton excited fluorescence for bioimaging. *Angewandte Chemie International Edition*, **2022**, *61* (31): e202206755.
- [13] Cui Y J, Li B, He H J, et al. Metal–organic frameworks as platforms for functional materials. *Accounts of Chemical Research*, **2016**, *49* (3): 483–493.
- [14] Li J Q, Li B, Yao X, et al. In situ coordination and confinement of two-photon active unit within metal–organic frameworks for high-order multiphoton-excited fluorescent performance. *Inorganic Chemistry*, **2022**, *61* (48): 19282–19288.
- [15] Wu Q, Du Q J, Sun X H, et al. MnMOF-based microwave-glutathione dual-responsive nano-missile for enhanced microwave Thermo-dynamic chemotherapy of drug-resistant tumors. *Chemical Engineering Journal*, **2022**, *439*: 135582.
- [16] Yan X Y, Pan Y X, Ji L, et al. Multifunctional metal–organic framework as a versatile nanoplatform for A β oligomer imaging and chemo-photothermal treatment in living cells. *Analytical Chemistry*, **2021**, *93* (41): 13823–13834.
- [17] Zhang X J, Chen Z K, Loh K P. Coordination-assisted assembly of 1-D nanostructured light-harvesting antenna. *Journal of the American Chemical Society*, **2009**, *131* (21): 7210–7211.
- [18] Guo X Y, Zhang M M, Qin J, et al. Revealing the effect of photothermal therapy on human breast cancer cells: a combined study from mechanical properties to membrane HSP70. *ACS Applied Materials & Interfaces*, **2023**, *15* (18): 21965–21973.
- [19] Yao X, Pei X X, Li B, et al. Rational fabrication of a two-photon responsive metal–organic framework for enhanced photodynamic therapy. *Inorganic Chemistry Frontiers*, **2021**, *8* (24): 5234–5239.
- [20] Zheng Y, Meana Y, Mazza M M A, et al. Fluorescence switching for temperature sensing in water. *Journal of the American Chemical Society*, **2022**, *144* (11): 4759–4763.
- [21] Tian Q W, Hu J Q, Zhu Y H, et al. Sub-10 nm Fe₃O₄@Cu_{2-x}S core–shell nanoparticles for dual-modal imaging and photothermal therapy. *Journal of the American Chemical Society*, **2013**, *135* (23): 8571–8577.